LETTERS

Resolvin D2 is a potent regulator of leukocytes and controls microbial sepsis

Matthew Spite[1], Lucy V. Norling[1,2], Lisa Summers[1], Rong Yang[1], Dianne Cooper[2], Nicos A. Petasis[3], Roderick J. Flower[2], Mauro Perretti[2] & Charles N. Serhan[1]

A growing body of evidence indicates that resolution of acute inflammation is an active process[1,2]. Resolvins are a new family of lipid mediators enzymatically generated within resolution networks that possess unique and specific functions to orchestrate catabasis, the phase in which disease declines[2,3]. Resolvin D2 (RvD2) was originally identified in resolving exudates, yet its individual contribution in resolution remained to be elucidated. Here, we establish RvD2's potent stereoselective actions in reducing excessive neutrophil trafficking to inflammatory loci. RvD2 decreased leukocyte–endothelial interactions *in vivo* by endothelial-dependent nitric oxide production, and by direct modulation of leukocyte adhesion receptor expression. In mice with microbial sepsis initiated by caecal ligation and puncture, RvD2 sharply decreased both local and systemic bacterial burden, excessive cytokine production and neutrophil recruitment, while increasing peritoneal mononuclear cells and macrophage phagocytosis. These multi-level pro-resolving actions of RvD2 translate to increased survival from sepsis induced by caecal ligation and puncture and surgery. Together, these results identify RvD2 as a potent endogenous regulator of excessive inflammatory responses that acts via multiple cellular targets to stimulate resolution and preserve immune vigilance.

Ungoverned inflammation is an underlying component of many pathologies, such as cardiovascular disease, diabetes and sepsis[4,5]. It's now recognized that resolution of inflammation is an active programme controlled by temporal and spatial production of specialized chemical mediators[2,3,6]. Recently, autacoids endogenously generated from omega-3 essential fatty acids, namely resolvins, were identified during the resolution phase of inflammation that actively promote catabasis via potent pro-resolving and anti-inflammatory actions[2,3]. RvD2, biosynthesized from docosahexaenoic acid (DHA), was originally identified during resolution[3]. Its complete stereochemistry and actions remained of interest. To this end, we investigated whether RvD2 preserves host immune function to facilitate resolution of inflammatory sepsis.

First, the complete stereochemistry of endogenous RvD2 was determined by physical matching with compounds prepared by total organic synthesis (Supplementary Fig. 1a) from enantiomerically and geometrically pure starting materials in accordance with the basic structure determined in resolving exudates[3] (Fig. 1). This approach was needed because the nanogram amounts of endogenous RvD2 isolated precluded direct nuclear magnetic resonance (NMR) analysis. The double-bond geometry of synthetic material was validated by ^{1}H NMR (Supplementary Fig. 1b). The biosynthesis of RvD2 involves 17-lipoxygenation of DHA to 17*S*-hydroperoxy-4*Z*, 7*Z*, 10*Z*, 13*Z*, 15*E*, 19*Z*-docosahexaenoic acid (17-HpDHA), which is enzymatically transformed to a 7(8)epoxide-containing intermediate[3,7] in human leukocytes. This enzymatic activity involves 5-lipoxygenase (LOX) and its epoxide-generating activity[8]. These steps can occur within a single cell type or via transcellular biosynthesis. For example, eosinophils, rich in 15-LOX, can convert DHA to 17-HpDHA, which polymorphonuclear neutrophils (PMNs) can convert to RvD2 (Fig. 1a). Actively phagocytosing PMNs converted resolvin precursor 17-HpDHA to RvD2 as determined by lipidomics based on liquid-chromatography tandem mass spectrometry (LC-MS/MS). A total ion chromatogram (mass-to-charge ratio $m/z = 375$ [M-H]) of human leukocyte-derived RvD2 is shown (Fig. 1b), with characteristic conjugated tetraene ultraviolet (UV)-chromophore (absorbance λ_{max} at 301 nm with shoulders at 289 nm and 315 nm). Synthetic material showed an exclusive and prominent peak with retention time and UV spectrum essentially identical to leukocyte-derived RvD2 (Fig. 1c). Co-injection of synthetic and leukocyte-derived RvD2 led to an increase in intensity and co-elution (Fig. 1d). To further establish the physical properties, their tandem mass spectra were analysed, with essentially identical mass spectrum, and diagnostic ions in agreement with original assignments for endogenous RvD2 (Fig. 1e, f)[3]. To validate the biosynthetic pathway, activated human PMNs were incubated with deuterium-labelled 17*S*-HpDHA-d_5 or DHA-d_5; RvD2 containing the d5 label was biosynthesized (Fig. 1g), the parent ion [M-H] increased to m/z 380, and neutral loss ions reflective of d5-containing fragments (Supplementary Fig. 2). Next, to further confirm the structural assignment[3,9], derivatized RvD2 was subjected to gas chromatography-mass spectrometry (GC/MS). The derivatized RvD2 C-value was 25.2 ± 0.1 and its spectrum (Supplementary Fig. 3) showed diagnostic ions at m/z 479, 435, 229 and 171 (see ref. 3). Collectively, matching of synthetic and leukocyte-derived RvD2 (by retention time, mass spectral diagnostic ions and derivatization) established the complete stereochemistry and double-bond geometry of endogenous RvD2 as 7*S*, 16*R*, 17*S*-trihydroxy-4*Z*, 8*E*, 10*Z*, 12*E*, 14*E*, 19*Z*-docosahexaenoic acid.

RvD2 displayed potent actions in microbial peritonitis, with a drastic ~70% reduction in zymosan-stimulated PMN infiltration at doses as low as 10 pg (Fig. 2). Importantly, the Δ10-*trans*-RvD2 isomer was essentially inactive, indicating that specific geometry of endogenous RvD2 is required for bioactivity. To determine whether RvD2 decreases leukocyte-endothelial interactions, microcirculation in the cremaster muscle was analysed. Platelet activating factor (PAF; 100 nM)[6,10] superfusion caused increased leukocyte adherence and emigration that was markedly reduced by 1 nM RvD2 (Fig. 2c, d). Representative microcirculation before and after RvD2 superfusion is shown in the Supplementary movies. These potent RvD2 actions were recapitulated with human cells to identify potential cellular directed actions (that is, endothelial cells and PMN). RvD2 potently reduced PAF-stimulated

[1]Center for Experimental Therapeutics and Reperfusion Injury, Department of Anesthesiology, Perioperative and Pain Medicine, Brigham and Women's Hospital and Harvard Medical School, Boston, Massachusetts 02115, USA. [2]William Harvey Research Institute, Barts and the London Medical School, Queen Mary University of London, London EC1M 6BQ, UK. [3]Department of Chemistry and Loker Hydrocarbon Research Institute, University of Southern California, Los Angeles, California 90089, USA.

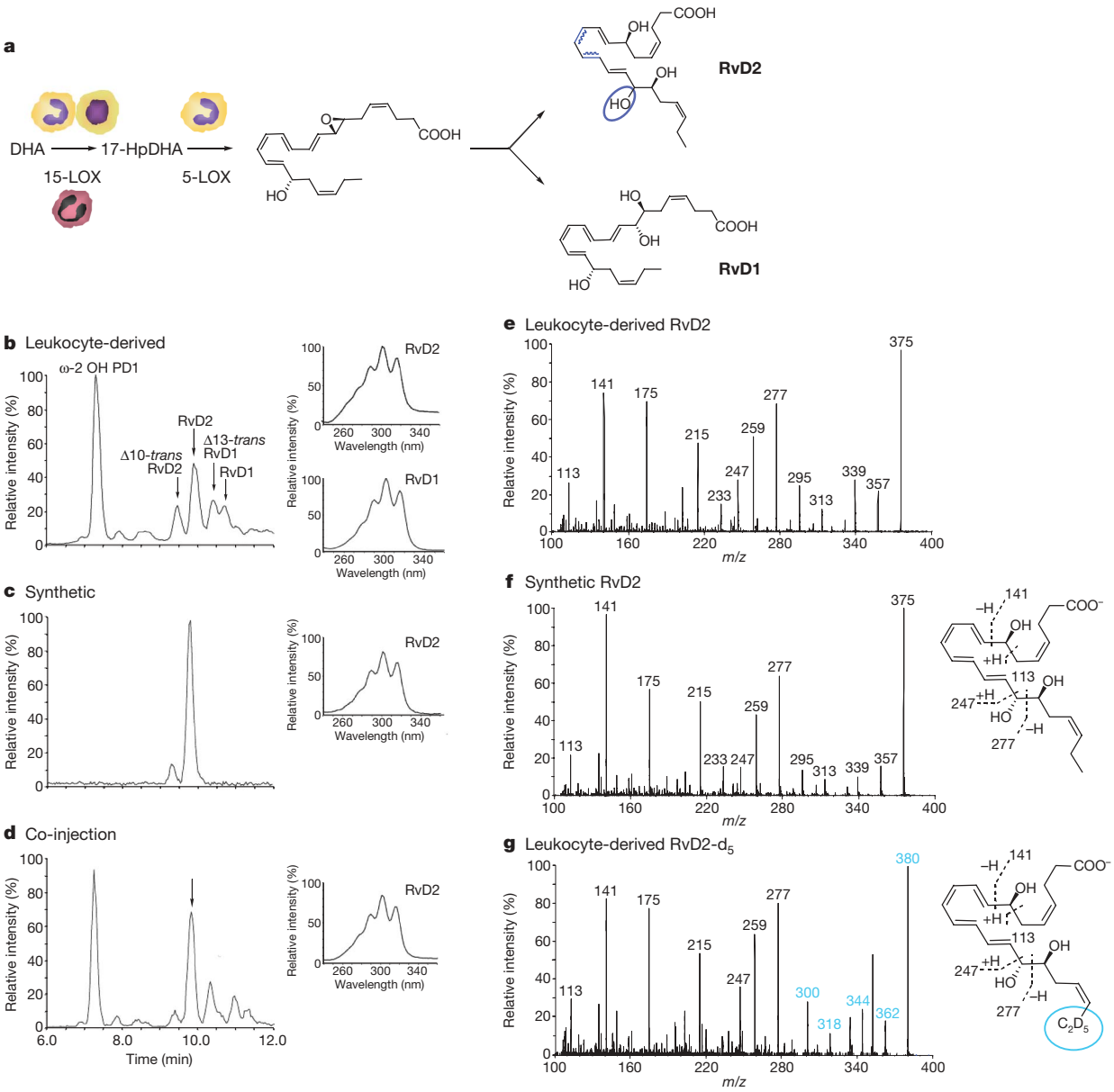

Figure 1 | Stereochemical assignment, biosynthesis and total organic synthesis of RvD2. **a**, Rv biosynthesis illustrating potential PMN and eosinophil transcellular biosynthesis. Blue, stereochemistries for assignments. **b**, Ion chromatograms (*m*/*z* 375) depicting human leukocyte-derived RvD2 and RvD1 with UV spectra (insets) and related isomers with the ω-2 OH metabolites of PD1 and 7,17-diHDHA. **c**, **d**, RvD2 prepared by total organic synthesis (**c**) and co-injection with leukocyte-derived RvD2 (**d**). **e**, **f**, MS/MS of leukocyte-derived RvD2 (**e**) and synthetic RvD2 (**f**) with prominent ions at *m*/*z* 357 [M-H-H_2O], 339 [M-H-2H_2O], 313 [M-H-CO_2-H_2O], 295 [M-H-CO_2-2H_2O], 277, 259 [277-H_2O], 247, 233 [277-CO_2], 141 and 113. **g**, Leukocyte-derived RvD2-d_5. Blue, d5-labelled ions. Representative of $n = 3$–5.

capture and adhesion of PMN by human umbilical vein endothelial cells (HUVECs) under flow (Supplementary Fig. 4)[11]. We note that RvD2 also reduced complement-mediated (with complement C5a) PMN–endothelial interactions (Supplementary Fig. 5a–c), a key mediator in sepsis[12]. Consistent with the impact of RvD2 on leukocyte–endothelial interactions, RvD2 diminished PAF-stimulated CD62L (L-selectin) shedding on isolated human PMN, and CD18 (ITGB2 , also known as integrin beta 2) surface expression (Fig. 2e, f). RvD2 alone did not alter PMN adhesion molecule expression ($n = 3$, not shown). To obtain further evidence for direct actions of RvD2 on human leukocytes, we monitored reactive oxygen species (ROS). Importantly, RvD2 did not stimulate extracellular superoxide, and it potently reduced C5a-stimulated extracellular superoxide generation (see below and Supplementary Fig. 5e, f).

Next, we assessed the contribution of nitric oxide, an established anti-adhesive mediator[13,14] in RvD2-reduced leukocyte adherence in post-capillary venules. The non-selective nitric oxide synthase inhibitor L-NAME, before addition of RvD2, partially reversed the decreased leukocyte adherence and emigration (Fig. 3a, b). To obtain additional evidence for nitric oxide generation by RvD2 *in vivo*, vascular fluorescence was monitored (see Methods). Topical administration of RvD2 (100 pg per ear) increased fluorescence intensity, whereas lower doses (1 pg and 10 pg) were ineffective (Supplementary Fig. 6a). L-NAME given before topical RvD2 application abolished this response (Supplementary Fig. 6b), indicating that RvD2-stimulated vascular responses at this dose were nitric-oxide-dependent. We note that intravenous injection of RvD2 at doses that inhibited PMN infiltration in peritonitis (10 pg) did not increase fluorescence intensity, indicating that only local elevated doses of RvD2 stimulated vascular responses (not shown). Additionally, RvD2 superfusion (1 nM) did not cause an increase in vascular permeability (Supplementary Fig. 6e). Topical RvD2 (10 pg or 100 pg) did not induce leukocyte infiltration into ear skin compared to chemoattractant leukotriene B_4 (Supplementary Fig. 6f). These results demonstrate that high focal delivery of RvD2 stimulates rapid

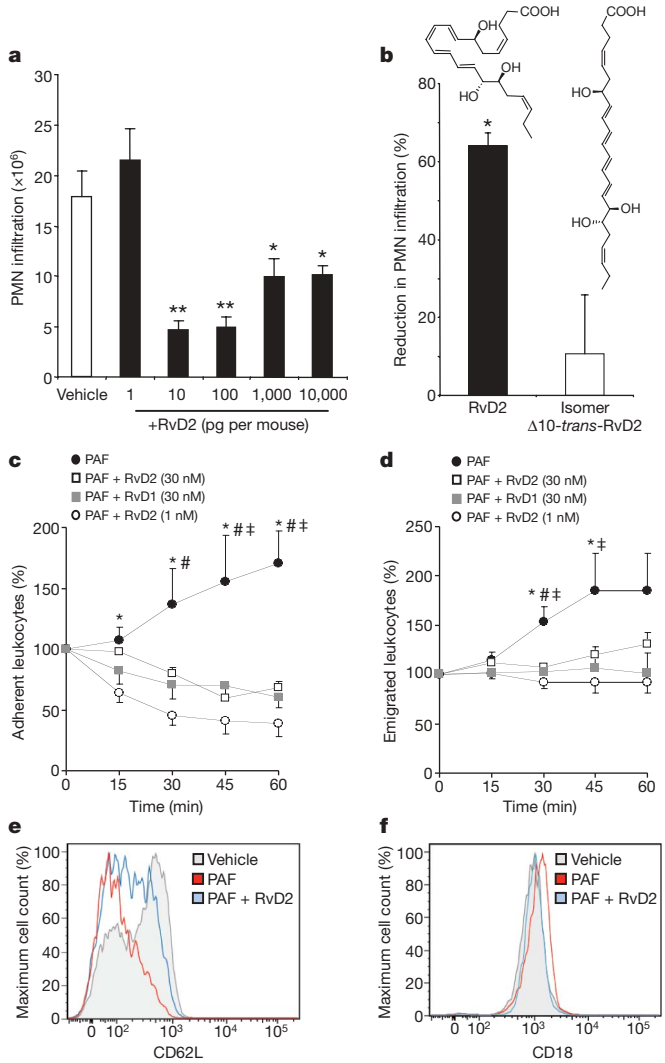

Figure 2 | RvD2 potently reduces leukocyte–endothelial interactions to reduce microbial peritonitis. **a**, **b**, Leukocyte infiltration in peritonitis. $*P < 0.05$, $**P < 0.01$ ANOVA. **b**, Equidose comparison (100 pg) of RvD2 and Δ10-*trans*-RvD2. **c**, **d**, Leukocyte trafficking *in vivo*. PAF-stimulated (100 nM) leukocyte adherence (**c**) and emigration (**d**) with or without RvD2 or RvD1. $*P < 0.01$ (PAF versus PAF + RvD2 1 nM), $\#P < 0.05$ (PAF versus PAF + RvD1 30 nM) and $\ddagger P < 0.05$ (PAF versus PAF + RvD2 30 nM) ANOVA. **e**, **f**, Adhesion receptor surface expression. Results ($n = 3$–6) are mean ± s.e.m.

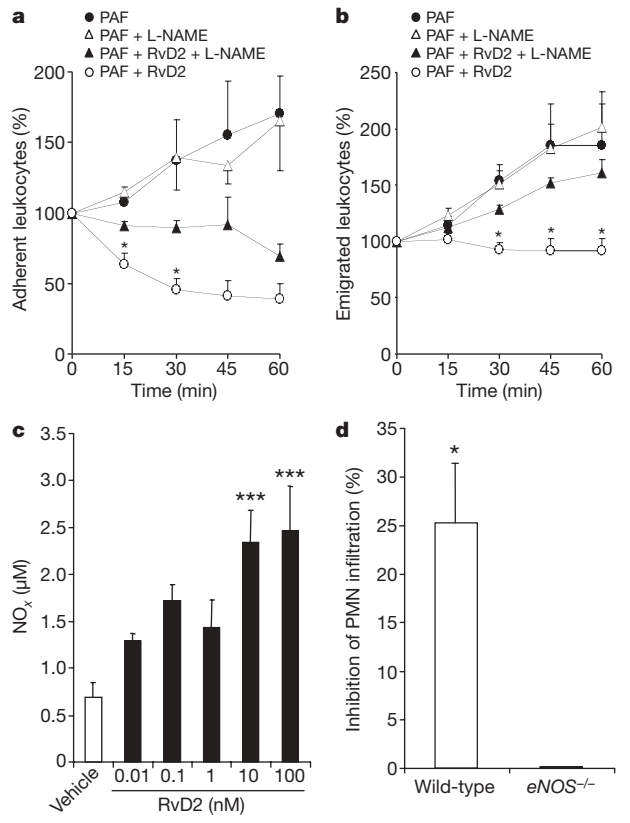

Figure 3 | Modulation of leukocyte trafficking by RvD2 is nitric oxide dependent. **a**, **b**, Leukocyte trafficking *in vivo*. Cremasters were superfused with PAF (100 nM), L-NAME (100 μM) and RvD2 (1 nM) and leukocyte adhesion (**a**) and emigration (**b**) was quantified ($n = 3$–5). $*P < 0.05$ two-way ANOVA. **c**, Nitric oxide (NO_x; nitrate or nitrite) generation in primary HUVECs incubated with RvD2 ($n = 4$–6). $***P < 0.001$, one-way ANOVA. **d**, Zymosan-stimulated PMN infiltration after administration of RvD2 (100 ng; intravenously) in wild-type and $eNOS^{-/-}$ mice ($n = 3$–5). Results are mean ± s.e.m. $*P < 0.05$, two-tailed unpaired Student's *t*-test.

nitric oxide production consistent with its anti-adhesive effects but not to a level that is pro-inflammatory.

Corroboratory results were obtained with HUVECs whereby RvD2 dose-dependently stimulated nitric oxide generation (Fig. 3c), suggesting that topical actions were probably mediated via endothelial nitric oxide synthase (eNOS). To test this, peritonitis was evaluated in mice deficient in eNOS. In agreement with an earlier report[15], no changes were observed with respect to leukocyte infiltration between wild-type and $eNOS^{-/-}$ (also known as $Nos3^{-/-}$) mice. RvD2 reduction in leukocytes was eliminated in $eNOS^{-/-}$ mice (Fig. 3d), an effect that has also been reported for aspirin and local aspirin-triggered lipoxins[16]. Notably, RvD2 also stimulated vasoprotective prostacyclin (6-keto-$PGF_{1\alpha}$; Supplementary Fig. 7a); this dose–response curve proved to be bell-shaped like other lipid mediators[1,2,6]. RvD2-stimulated prostacyclin and nitric oxide were sensitive to pertussis toxin, implicating a role for G-protein coupled receptor(s) (Supplementary Fig. 7b, c). Thus, RvD2 regulates leukocyte adherence via both direct actions on PMN (see above) and endothelial vasoactive substances.

Next, anti-inflammatory and pro-resolving actions of RvD2 were evaluated in caecal ligation and puncture (CLP), an established murine microbial sepsis that closely resembles human pathology[17,18]. Omega-3 fatty acids are beneficial in some inflammatory conditions, including sepsis[19–21], although the mechanistic basis underlying protection is still emerging. Indeed, RvD2 significantly reduced the amount of live aerobic bacteria in both blood and peritoneum at 12 h post-CLP, whereas Δ10-*trans*-RvD2 was essentially not active (Fig. 4a, b). This was associated with a significant reduction in total leukocytes and specifically, PMN infiltration into the peritoneum (Fig. 4c, d). Interestingly, the ratio of mononuclear cells to PMN was increased with RvD2 (Fig. 4d, inset), similar to results obtained with sterile zymosan-stimulated peritonitis (Supplementary Fig. 9a). Intraperitoneal delivery of RvD2 at 1 h post-CLP also reduced both blood and peritoneal bacteria (Supplementary Fig. 8). Macrophages have an important role in the clearance of bacteria, cellular debris and apoptotic PMNs to facilitate inflammation resolution[1,2]. RvD2 treatment promoted phagocyte-dependent bacterial clearance observed in inguinal lymph nodes (Supplementary Fig. 10d). Evidence for direct macrophage actions were obtained *in vitro*, where RvD2 potently enhanced macrophage phagocytosis of opsonized-zymosan (Supplementary Fig. 9b).

To obtain additional evidence for this pro-resolution role of RvD2, cytokines were monitored during CLP both locally (peritoneum) and systemically (plasma). RvD2 drastically reduced levels of pro-inflammatory cytokines associated with poor outcomes in sepsis[18], namely the interleukins IL-6, IL-1β, IL-23 and tumour necrosis factor TNF-α (Fig. 4e and Supplementary Fig. 10a). RvD2 reduced cytokine levels while enhancing bacterial clearance, a response also observed for macrophage scavenger receptor A[22]. Hence, it

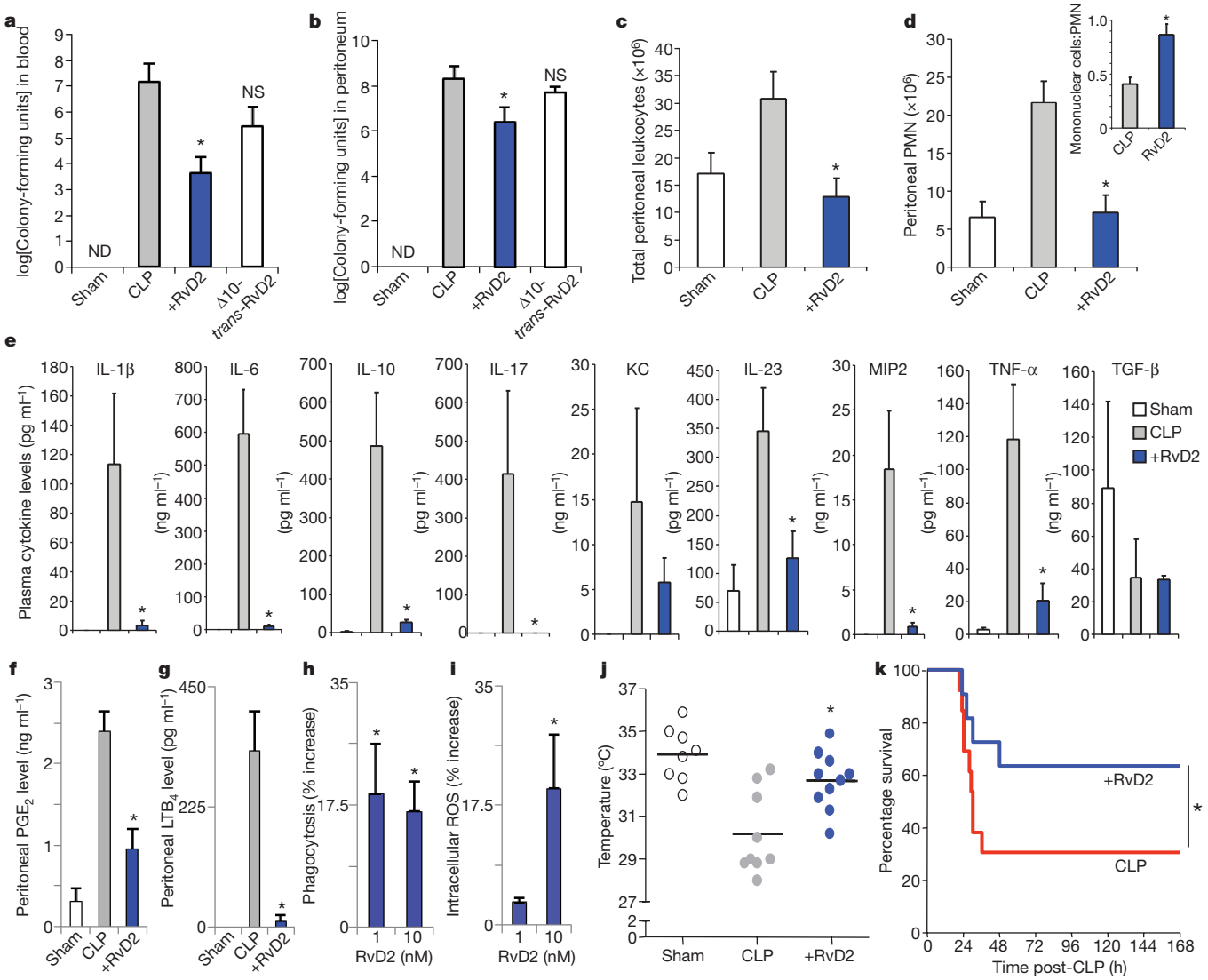

Figure 4 | RvD2 reduces bacterial levels, systemic inflammation and enhances survival in microbial sepsis. **a**, **b**, Aerobic bacteria levels in blood (**a**) and peritoneal exudates (**b**) from sham or CLP-operated mice ± RvD2 methyl ester (RvD2-Me) (100 ng; intravenously) at 12 h ($n = 5$–6 per group). ND, not detected; NS, not significant. **c**, **d**, Peritoneal leukocyte differentials, ratio of mononuclear to polymorphonuclear cells inset. ($n = 3$–5). **e**, Plasma cytokine levels ($n = 3$–6). **f**, **g**, Peritoneal PGE_2 and LTB_4 levels. **h**, **i**, Phagocytosis of *E. coli* and intracellular ROS in human PMN. **j**, Temperatures of mice 12 h post-CLP. **k**, Kaplan–Meier survival analysis of vehicle- ($n = 13$) and RvD2-treated ($n = 12$) CLP mice. Results are mean ± s.e.m. **a**–**g**, $^*P < 0.05$ two-tailed unpaired Student's *t*-test. **h**, **j**, $^*P < 0.05$ by one-way ANOVA. **k**, $^*P < 0.05$ one-tailed log-rank test.

is plausible that RvD2 prevents persistent amplification signals downstream of pattern-recognition receptors, dampening the responses of classically activated macrophages[23,24].

RvD2 also drastically decreased IL-17, as well as IL-10, which is of interest because of its detrimental impact on survival in sepsis[25]. Thus, RvD2 differs in action from lipoxin A_4, which stimulates IL-10 (ref. 26). High levels of both pro- and anti-inflammatory cytokines, including IL-10, are predictive of early mortality in sepsis, and diminishing IL-10 levels proved beneficial in sepsis[27,28]. Pro-inflammatory mediators, including prostaglandin E_2 (PGE_2) and LTB_4, were also decreased in peritoneum by RvD2 (Fig. 4f, g and Supplementary Fig. 10b, c). Interestingly, in addition to macrophage-directed actions, RvD2 directly enhanced PMN *Escherichia coli* phagocytosis that was accompanied by an increase in intracellular ROS (Fig. 4h, i). RvD2 does not possess direct antibacterial activity compared to ampicillin (Supplementary Fig. 11). RvD2-treated CLP mice also showed protection at 12 h post-CLP from hypothermia (Fig. 4j). Accordingly, RvD2 dramatically increased survival rates among CLP-operated mice (Fig. 4k) and activity levels 12 h post-CLP were resumed (Supplementary movie 3).

The present results establish the complete stereochemistry of endogenous RvD2 and its potent stereoselective actions facilitating resolution. Local and systemic bacterial burden in microbial sepsis were controlled and significantly dampened with RvD2. This potent D-series resolvin protected CLP-mice from excessive leukocyte infiltration and overzealous cytokine production, and also enhanced clearance of microbes, thus preventing sepsis-induced lethality. Sepsis remains a clinical challenge, with high mortality rates and increasing prevalence[5,29]. Given the uncontrolled inflammatory pathogenesis of sepsis, anti-inflammatory therapies are used for sepsis management in humans, but have ultimately failed owing primarily to sustained immunosuppression[5]. Overall, these results indicate that RvD2 is a potent endogenous mediator which actively promotes the resolution of inflammation, suggesting new therapeutic approaches that do not compromise host defence.

METHODS SUMMARY

Intra-vital microscopy. Experiments were approved by and performed under guidelines of the Ethical Committee for Use of Animals, Barts and The London School of Medicine and Home Office regulations (Guidance on the Operation of

Animals, Scientific Procedures Act, 1986). Intra-vital microscopy was used to observe actions of RvD2 on leukocyte responses stimulated by PAF (100 nM C16 form $C_{26}H_{54}NO_7P$; Sigma; PAF administered 1 h before RvD2 was given at time 0) within the cremasteric microcirculation of C57 BL/6 mice. Mice were anaesthetized with xylazine (7.5 mg kg^{-1}) and ketamine (150 mg kg^{-1}), and cremaster prepared[30]. In some experiments, fluorescein isothiocyanate (FITC)-albumin (1 mg) was administered intravenously to assess vascular leakage.

Caecal ligation and puncture. CLP was performed in male FVB mice[17], in accordance with the Harvard Medical Area Standing Committee On Animals Protocol #02570. The caecum was ligated below the ileocaecal valve for mid-grade sepsis[17]. A through and through puncture was performed with a 20-gauge needle, followed by one additional puncture in the distal tip of the caecum. Mice received saline (500 µl subcutaneously) followed by intravenous administration of vehicle (0.1% ethanol), or RvD2 methyl ester (100 ng) at the time of puncture. In some experiments, RvD2-Me (1 µg) was administered intraperitoneally 1 h post-CLP. At 12 h, rectal temperature was measured, blood collected by cardiac puncture and peritoneal exudates obtained. Blood and peritoneal bacteria levels were determined by growth on tryptic soy agar plates. Plasma and peritoneal cytokine levels were determined by Searchlight array. Peritoneal cells were differentiated using Wright-Giemsa staining.

Statistics. Data are mean ± s.e.m. Multiple group comparisons were made using one-way or two-way analysis of variance (ANOVA) followed by Dunnett's or Bonferroni post tests where appropriate and direct comparisons made using a two-tailed unpaired Student's *t*-test. Kaplan–Meier survival curves were analysed using a one-tailed log-rank test. In all cases, a P value <0.05 was considered significant.

Full Methods and any associated references are available in the online version of the paper at www.nature.com/nature.

Received 18 August; accepted 21 September 2009.

1. Gilroy, D. W., Lawrence, T., Perretti, M. & Rossi, A. G. Inflammatory resolution: new opportunities for drug discovery. *Nature Rev. Drug Discov.* **3,** 401–416 (2004).
2. Serhan, C. N., Chiang, N. & Van Dyke, T. E. Resolving inflammation: dual anti-inflammatory and pro-resolution lipid mediators. *Nature Rev. Immunol.* **8,** 349–361 (2008).
3. Serhan, C. N. *et al.* Resolvins: a family of bioactive products of omega-3 fatty acid transformation circuits initiated by aspirin treatment that counter proinflammation signals. *J. Exp. Med.* **196,** 1025–1037 (2002).
4. Weber, C., Zernecke, A. & Libby, P. The multifaceted contributions of leukocyte subsets to atherosclerosis: lessons from mouse models. *Nature Rev. Immunol.* **8,** 802–815 (2008).
5. Hotchkiss, R. S. & Karl, I. E. The pathophysiology and treatment of sepsis. *N. Engl. J. Med.* **348,** 138–150 (2003).
6. Shimizu, T. Lipid mediators in health and disease: enzymes and receptors as therapeutic targets for the regulation of immunity and inflammation. *Annu. Rev. Pharmacol. Toxicol.* **49,** 123–150 (2009).
7. Hong, S., Gronert, K., Devchand, P. R., Moussignac, R. L. & Serhan, C. N. Novel docosatrienes and 17S-resolvins generated from docosahexaenoic acid in murine brain, human blood, and glial cells. Autacoids in anti-inflammation. *J. Biol. Chem.* **278,** 14677–14687 (2003).
8. Shimizu, T., Radmark, O. & Samuelsson, B. Enzyme with dual lipoxygenase activities catalyzes leukotriene A4 synthesis from arachidonic acid. *Proc. Natl Acad. Sci. USA* **81,** 689–693 (1984).
9. Rodriguez, A. R. & Spur, B. W. First total synthesis of 7(S),16(R),17(S)-Resolvin D2, a potent anti-inflammatory lipid mediator. *Tetrahedr. Lett.* **45,** 8717–8720 (2004).
10. Prescott, S. M., Zimmerman, G. A., Stafforini, D. M. & McIntyre, T. M. Platelet-activating factor and related lipid mediators. *Annu. Rev. Biochem.* **69,** 419–445 (2000).
11. Cooper, D., Norling, L. V. & Perretti, M. Novel insights into the inhibitory effects of Galectin-1 on neutrophil recruitment under flow. *J. Leukoc. Biol.* **83,** 1459–1466 (2008).
12. Rittirsch, D. *et al.* Functional roles for C5a receptors in sepsis. *Nature Med.* **14,** 551–557 (2008).
13. Kubes, P., Suzuki, M. & Granger, D. N. Nitric oxide: an endogenous modulator of leukocyte adhesion. *Proc. Natl Acad. Sci. USA* **88,** 4651–4655 (1991).
14. Moncada, S. & Higgs, E. A. The discovery of nitric oxide and its role in vascular biology. *Br. J. Pharmacol.* **147** (Suppl. 1), S193–S201 (2006).
15. Bucci, M. *et al.* Endothelial nitric oxide synthase activation is critical for vascular leakage during acute inflammation *in vivo*. *Proc. Natl Acad. Sci. USA* **102,** 904–908 (2005).
16. Paul-Clark, M. J., Van Cao, T., Moradi-Bidhendi, N., Cooper, D. & Gilroy, D. W. 15-epi-lipoxin A4-mediated induction of nitric oxide explains how aspirin inhibits acute inflammation. *J. Exp. Med.* **200,** 69–78 (2004).
17. Rittirsch, D., Huber-Lang, M. S., Flierl, M. A. & Ward, P. A. Immunodesign of experimental sepsis by cecal ligation and puncture. *Nature Protocols* **4,** 31–36 (2009).
18. Buras, J. A., Holzmann, B. & Sitkovsky, M. Animal models of sepsis: setting the stage. *Nature Rev. Drug Discov.* **4,** 854–865 (2005).
19. Singer, P. *et al.* Anti-inflammatory properties of omega-3 fatty acids in critical illness: novel mechanisms and an integrative perspective. *Intensive Care Med.* **34,** 1580–1592 (2008).
20. Farolan, L. R., Goto, M., Myers, T. F., Anderson, C. L. & Zeller, W. P. Perinatal nutrition enriched with omega-3 polyunsaturated fatty acids attenuates endotoxic shock in newborn rats. *Shock* **6,** 263–266 (1996).
21. Pluess, T. T. *et al.* Intravenous fish oil blunts the physiological response to endotoxin in healthy subjects. *Intensive Care Med.* **33,** 789–797 (2007).
22. Haworth, R. *et al.* The macrophage scavenger receptor type A is expressed by activated macrophages and protects the host against lethal endotoxic shock. *J. Exp. Med.* **186,** 1431–1439 (1997).
23. Litvak, V. *et al.* Function of C/EBPdelta in a regulatory circuit that discriminates between transient and persistent TLR4-induced signals. *Nature Immunol.* **10,** 437–443 (2009).
24. Mosser, D. M. & Edwards, J. P. Exploring the full spectrum of macrophage activation. *Nature Rev. Immunol.* **8,** 958–969 (2008).
25. Flierl, M. A. *et al.* Adverse functions of IL-17A in experimental sepsis. *FASEB J.* **22,** 2198–2205 (2008).
26. Souza, D. G. *et al.* The required role of endogenously produced lipoxin A4 and annexin-1 for the production of IL-10 and inflammatory hyporesponsiveness in mice. *J. Immunol.* **179,** 8533–8543 (2007).
27. Osuchowski, M. F., Welch, K., Siddiqui, J. & Remick, D. G. Circulating cytokine/inhibitor profiles reshape the understanding of the SIRS/CARS continuum in sepsis and predict mortality. *J. Immunol.* **177,** 1967–1974 (2006).
28. Huang, X. *et al.* PD-1 expression by macrophages plays a pathologic role in altering microbial clearance and the innate inflammatory response to sepsis. *Proc. Natl Acad. Sci. USA* **106,** 6303–6308 (2009).
29. Dombrovskiy, V. Y., Martin, A. A., Sunderram, J. & Paz, H. L. Rapid increase in hospitalization and mortality rates for severe sepsis in the United States: a trend analysis from 1993 to 2003. *Crit. Care Med.* **35,** 1244–1250 (2007).
30. Chatterjee, B. E. *et al.* Annexin 1-deficient neutrophils exhibit enhanced transmigration *in vivo* and increased responsiveness *in vitro*. *J. Leukoc. Biol.* **78,** 639–646 (2005).

Supplementary Information is linked to the online version of the paper at www.nature.com/nature.

Acknowledgements We acknowledge support from National Institutes of Health grants GM-38765 and P50-DE016191 (C.N.S.), Welcome Trust Programme grant 086867/Z/08/Z (R.J.F. and M.P.) and Project grant 085903/Z/08 (R.J.F.) and Arthritis Research Campaign UK fellowships 18445 and 18103 (to L.V.N. and D.C., respectively). M.S. received a National Research Service Award from the NHLBI (HL087526). We thank J. W. Winkler and J. Uddin for work related to RvD2 synthesis, P. Pillai, K. Martinod, G. Fredman and J. Dalli for technical assistance, and M. H. Small for assistance with the manuscript. We also thank B. Schmidt for histopathology, Children's Hospital Boston.

Author Contributions M.S. and L.V.N. designed and carried out experiments, analysed data and wrote the manuscript; L.S., R.Y. and D.C. carried out experiments and analysed data; N.A.P. synthesized RvD2; R.J.F. and M.P. designed experiments, analysed data and contributed to the manuscript; C.N.S. planned the project, designed experiments, analysed data and wrote the manuscript.

Author Information Reprints and permissions information is available at www.nature.com/reprints. The authors declare competing financial interests: details accompany the full-text HTML version of the paper at www.nature.com/nature. Correspondence and requests for materials should be addressed to C.N.S. (cnserhan@zeus.bwh.harvard.edu).

METHODS

RvD2 total organic synthesis. Total organic synthesis of RvD2 will be reported elsewhere. Briefly, stereochemically pure RvD2 methyl ester was prepared using chiral starting materials having the same stereochemistry of the three OH groups and using stereochemically controlled processes (Supplementary Fig. 1a). Thus, the synthesis started with the nucleophilic opening of enantiomerically pure protected glycidol **1** with a protected derivative of pentynoic acid **2**, followed by functional group manipulations to form intermediate **3**. Synthesis of the intermediate that contains the 16,17-diol moiety was prepared starting with a protected form of 2-deoxyribose **4**, which was converted to intermediate **5** using a Wittig reaction that selectively formed a C = C bond with a Z-geometry. Conversion of **5** to alkyne intermediate **6**, followed by palladium-mediated Sonogashira coupling of **6** with iodide **3** gave compound **7**, the acetylenic precursor of RvD2. Removal of the protective groups and selective hydrogenation to convert the alkyne moiety to a C = C bond with a Z-geometry gave the RvD2 methyl ester (RvD2-Me). This compound was purified by high-performance liquid chromatography (HPLC) and fully characterized with NMR spectroscopy and mass spectrometry (Supplementary Fig. 1 and Fig. 1c and f). This is a different synthetic strategy for RvD2 than reported in ref. 9. The Δ10-*trans*-RvD2 was prepared by isomerization at room temperature (21 °C) and exposure to light overnight, and was isolated using reverse phase (RP)-HPLC before bioassay.

RvD2 biosynthesis. Isolated human PMNs were isolated from healthy volunteers (BWH protocol # 88-02462) suspended in DPBS+/+ (25×10^6 cells ml^{-1}) and incubated with 5 μg 17*S*-hydroperoxy-4*Z*,7*Z*,10*Z*,13*Z*,15*E*,19*Z*-docosahexaenoic acid (17-HpDHA) and/or 17-HDHA and stimulated with zymosan (100 μg) or A23187 (5 μM) for 30 min at 37 °C (ref. 3). Incubations were stopped with cold methanol and samples were solid-phase extracted[31].

Mediator lipidomics. LC/UV/MS/MS-based mediator lipidomic analysis was performed with an HPLC (Shimadzu LC20AD) connected inline with a UV diode array detector (Agilent G1315B), coupled to a hybrid quadrupole time-of-flight mass spectrometer (QStar XL; Applied Biosystems) equipped with a Phenomenex Luna C18(2) column (2 mm × 150 mm × 3 μm). Acquisition was carried out in negative ionization mode. The mobile phase consisted of methanol/water/acetic acid (60:40:0.01, v/v/v) and was ramped to 85:15:0.01 over 30 min and to 100:0:0.01 over the next 5 min at a flow rate of 200 μl min^{-1}. The flow rate was increased to 400 μl min^{-1} over the next 10 min. The operating parameters were: gas1 35.00, gas2 55.00, curtain gas 40, electrospray voltage –4,200 V, evaporation temperature 400 °C, decluster potential –35 V, and collision energies were optimized individually. GC/MS analysis was carried out with an HP 6890 gas chromatography system equipped with an HP-5MS capillary column (0.25 mm inner diameter × 30 m, Agilent) and an HP5973 mass selective detector (Hewlett-Packard)[31].

Targeted LC-MS/MS-based lipidomics of CLP exudates. Exudate lavages (2 ml) were collected and immediately added to 2 volumes of cold methanol for extraction and work-up as in ref. 31. LC-MS/MS identification was acquired with an Agilent 1100 series HPLC paired with an ABI Sciex Instruments 3200 Q TRAP linear ion trap quadrupole mass spectrometer. The column (Agilent Eclipse Plus C18, 4.6 mm × 50 mm × 1.8 μm) was eluted at a flow rate of 0.4 ml min^{-1} with methanol/water/acetic acid (60/40/0.01;v/v/v) ramped to 80/20/0.01 (v/v/v) after 5 min, 95/5/0.01 (v/v/v) after 8 min, and 100/0/0.01 after 14 min to wash the column. Instrument control and data acquisition were performed using Analyst 1.4.2 software. Ion pair transitions from previously reported multiple reaction monitoring methods were used for profiling and quantitation of PGE_2 (351.2/189.2) and LTB_4 (335.2/195.2). Criteria for identification were: liquid chromatography retention time and a minimum of six fragment diagnostic ions on the MS/MS spectrum matching those of synthetic standards. Deuterated 5S-HETE (Cayman Chemicals, 2 ng) was added before extraction as internal standard for recovery calculations.

Murine peritonitis and macrophage phagocytosis. Peritonitis was assessed using male FVB mice (Charles River) or *eNOS*$^{-/-}$ mice and their wild-type littermates (C57BL/6J; Jackson Labs). Vehicle (1.0% EtOH) or RvD2 (0.001–100 ng per mouse) were administered intravenously followed by intraperitoneal administration of zymosan A (1 mg; Sigma). Peritoneal lavages were collected after 4 h and leukocyte infiltration was assessed by light microscopy, followed by differential analysis using Wright–Giemsa staining. For macrophage phagocytosis, resident peritoneal macrophages were harvested from naive mice and incubated with RvD2 (0.01–100 nM) for 15 min at 37 °C before the addition of opsonized FITC-labelled zymosan. After 30 min, extracellular fluorescence was quenched by trypan blue and fluorescence was determined using a Victor3 plate reader (PerkinElmer).

Direct actions of RvD2 on human endothelial cells and PMN. Primary HUVECs (Lonza) were incubated with or without pertussis toxin (100 ng ml^{-1}, 12 h) with vehicle alone (0.1% EtOH) or RvD2 (0.01–100.0 nM) for 30 min at 37 °C and supernatants were analysed for NO_x (nitrate or nitrite) by the Greiss reaction (Biomol) and 6-keto $PGF_{1\alpha}$ by ELISA (Neogen). Human PMN were isolated from healthy donors by Ficoll gradient and incubated with PAF (1 nM) with or without RvD2 (0.01–10 nM) for 15 min at 37 °C and the surface expression of CD62L and CD18 was determined by flow cytometry using phycoerythrin-conjugated anti-CD18 (6.7) and FITC-conjugated anti-CD62L (Dreg 56; BD Biosciences) or appropriate isotype control (IgG1κ). To assess leukocyte–endothelial interactions, the flow chamber assay was used[11], human PMN were stimulated before flow with PAF (1 nM) or C5a (0.1 nM) for 15 min.

Extracellular superoxide assay. PMN were incubated with 5 μM lucigenin in a thermostatted (37 °C) luminometer (Wallac VICTOR2 1420 Multilabel Counter, Perkin Elmer). After 15 min, PMN were treated with vehicle, C5a (10 nM) or RvD2 (1–10 nM) and monitored for 20 min. Alternatively, PMN were incubated with RvD2 (1–10 nM) for 15 min before vehicle or C5a (10 nM).

Assessment of *in vivo* vascular responses by fluorescence imaging. Male FVB mice (6–8 weeks) were anaesthetized with pentobarbital (50 mg kg^{-1}, intraperitoneally) and injected intravenously with FITC-albumin (2.5 mg) alone or plus L-NAME (24 mg kg^{-1}). Acetone or RvD2-methyl ester (20 μl at indicated doses) was applied to the inner ear. Fluorescence was assessed using the Night Owl LB 981 NC 320 Molecular Light Imager (Berthold Technologies) and images were acquired for 1,500 ms (every 5 min) using a HQ 475 excitation filter (Chroma) and Winlight Software. The mean change in fluorescence intensity was normalized to acetone control. In some experiments, RvD2 (10 pg; intravenously) was administered in conjunction with FITC-albumin.

In separate experiments, topical application of LTB_4 (1.0 μg; Cayman), RvD2-Me (0.1 or 0.01 ng) or acetone were applied to the inner ear. After 24 h, 6 mm punch biopsies were obtained, flash frozen in liquid N_2, stored at −80 °C and myeloperoxidase activity was assessed as in ref. 32.

***E. coli* phagocytosis and generation of intracellular ROS.** Adherent human PMN were pre-incubated with RvD2 (0.1–100 nM) or vehicle for 15 min before incubation with *E. coli* (JM109; 50:1 ratio) at 37 °C for 60 min. PMN were rinsed, fixed and permeabilized (BD Cytofix/Cytoperm; BD Biosciences), and *E. coli* levels were assessed using FITC-conjugated anti-*E. coli* antibody (GTX40856; GeneTex) by flow cytometry. To assess intracellular ROS generation, PMN were incubated with 5 μM carboxy-H2DCFDA (C400; Invitrogen) for 30 min before incubation with RvD2 and *E. coli*, and probe oxidation was determined using a Victor3 plate reader (Perkin Elmer).

Antibacterial susceptibility test. Mid-logarithmic phase *E. coli* (5×10^7 colony-forming units) was inoculated on LB agar plates, discs containing RvD2 (0.1–100 ng) or ampicillin (10 μg) were placed on top, and the zone of clearing was assessed after overnight incubation.

Immunohistochemistry. Inguinal lymph nodes and spleens were excised 12 h after CLP and fixed in 3% formalin. Tissues were paraffin-embedded, sectioned and slides were stained with haematoxylin and eosin and Gram by the Department of Pathology at the Children's Hospital Boston.

31. Serhan, C. N., Lu, Y., Hong, S. & Yang, R. Mediator lipidomics: search algorithms for eicosanoids, resolvins, and protectins. *Methods Enzymol.* **432**, 275–317 (2007).

32. Takano, T., Clish, C. B., Gronert, K., Petasis, N. & Serhan, C. N. Neutrophil-mediated changes in vascular permeability are inhibited by topical application of aspirin-triggered 15-epi-lipoxin A4 and novel lipoxin B4 stable analogues. *J. Clin. Invest.* **101**, 819–826 (1998).